



Dispersion and hydrogenation activity of surfactant-stabilized Rh(0) nanoparticles prepared on different mesoporous supports

Maya Boutros^{a,b}, Guillaume Shirley^a, Thomas Onfroy^{a,c}, Franck Launay^{a,c,*}

^a UPMC Univ Paris 6, Laboratoire des Systèmes Interfaciaux à l'Echelle Nanométrique, CNRS UMR 7142, 4 place Jussieu, 75252 Paris Cedex 05, France

^b Université Libanaise, Faculté des Sciences II, Laboratoire de Chimie Physique des Matériaux (LCPM), Campus Fanar, BP 90656, Jdeidh, Lebanon

^c UPMC Univ Paris 6, Laboratoire de Réactivité de Surface, CNRS UMR 7197, 4 place Jussieu, 75252 Paris Cedex 05, France

ARTICLE INFO

Article history:

Received 4 October 2010

Received in revised form

21 December 2010

Accepted 27 December 2010

Available online 4 January 2011

Keywords:

Rh(0) nanoparticles

SBA-15

CMK-3

Hydrogenation

Aromatic substrates

ABSTRACT

Supported Rh(0) colloidal particles were prepared by the reduction of Rh(III) ions by sodium borohydride in the presence of N,N-dimethyl-N-cetyl-N-(2-hydroxyethyl) ammonium chloride (HEA16Cl), usually used as a stabilizing agent in solution. Tested supports were Na–Al–SBA-15, SBA-15 and CMK-3. In each case, the influence of HEA16Cl was studied by comparison with blank samples. Surfactant and rhodium uptake were evaluated by means of elemental analysis and eventually thermogravimetry. Obtained materials were also characterized by XRD, N₂ sorption and TEM. Given the results, it appears that HEA16Cl promotes rhodium uptake in all cases. Most significant effects on the size and dispersion of particles were observed for the system combining HEA16Cl and Na–Al–SBA-15. All the solids prepared in this study were tested in the room temperature hydrogenation of styrene as well as that of a more demanding substrate, diphenylmethane, at 0.1 MPa of H₂. All of them were generally more active than their commercial analogue (5 wt.% Rh⁰/C). Best catalysts, i.e., those prepared from Na–Al–SBA-15 in the presence of HEA16Cl as well as CMK-3 without HEA16Cl, allowed almost 100% yield of dicyclohexylmethane within 6 h (molar substrate/Rh = 100).

© 2011 Elsevier B.V. All rights reserved.

1. Introduction

Controlled nanometer-sized metal particles have received considerable attention in both industry and academia due to their superior physical and chemical properties compared with bulk materials [1–5]. One of the strategies to take advantage of these properties for catalysis applications is based on the deposition of nanostructured metal colloids onto supports with high specific surface area and narrow pore size distribution. Structured mesoporous materials are good candidates to obtain a high dispersion degree of the metal and improved accessibility of active sites in comparison to supports like zeolites [6–15]. At this time, mesoporous materials including SBA-15 and carbon CMK-3 have been already used as host structures for preformed metal nanoparticles [16–32], and some research efforts have been focused on their applications as heterogeneous catalysts. Insertion of stabilized colloidal nanoparticles in the mesopore network is usually performed by their

deposition onto preformed materials [16–23,30,31] or their introduction in the synthesis gel of the support [24–32]. However, the relatively low amount of metal introduced and the difficulty in inserting the particles homogeneously within the porosity are important drawbacks of these approaches.

Another pathway proposed by our group consists to prepare the colloids directly onto the support. Indeed, we showed previously [33] that well-dispersed Rh(0) particles can be obtained by the reduction of Rh(III)-exchanged mesoporous aluminosilicates (Na–Al–SBA-15) by sodium borohydride in the presence of a water soluble stabilizing agent, N,N-dimethyl-N-cetyl-N-(2-hydroxyethyl) ammonium chloride (HEA16Cl). The efficiency of this strategy was attributed first to the combined use of an acidic support, Al–SBA-15, and of a quaternary ammonium salt, HEA16Cl. The present paper aims at comparing various hexagonally ordered siliceous or non siliceous materials in order to emphasize the effect of the support nature and the role of HEA16Cl on the location, the size of the nanoparticles and their catalytic activity in arene hydrogenation under mild conditions. For this purpose, Rh(0)-containing mesoporous SBA-15, Al–SBA-15 and CMK-3 were synthesized in the presence or in the absence of HEA16Cl molecules. The resulting solids were characterized by thermogravimetric analysis (TGA), X-ray diffraction, nitrogen sorption and transmission

* Corresponding author at: UPMC Univ Paris 6, Laboratoire de Réactivité de Surface, CNRS UMR 7197, 4, place Jussieu, 75252 Paris Cedex 05, France.
Tel.: +33 1 44 27 58 75; fax: +33 1 44 27 60 33.

E-mail address: franck.launay@upmc.fr (F. Launay).

electron microscopy (TEM). The different solids were also tested as catalysts in the room temperature hydrogenation of styrene and diphenylmethane under 0.1 MPa dihydrogen pressure.

2. Experimental methods

2.1. Materials synthesis

The different reagents, i.e., rhodium chloride hydrate ($\text{RhCl}_3 \cdot x\text{H}_2\text{O}$, 40.8% Rh, $x=2.25$, Strem), sodium borohydride (NaBH_4 , 99%, Aldrich), aluminium isopropoxide ($\text{Al}[(\text{CH}_3)_2\text{CHO}]_3$, 98%, Aldrich), Pluronic P123 ($(\text{EO})_{20}(\text{PO})_{70}(\text{EO})_{20}$, $M_{\text{av}}=5800$, Aldrich), tetraethyl orthosilicate (TEOS, $\geq 99\%$, Fluka), tetramethyl orthosilicate (TMOS, $\geq 99\%$, Fluka), 37 wt.% fuming hydrochloric acid (SDS), 98 wt.% sulfuric acid (Carlo Erba), sucrose ($>99.5\%$, Sigma), NaCl (99.9%, Carlo Erba), 30 wt.% aqueous ammonia (Carlo/Erba), were used as received. N,N-dimethyl-N-cetyl-N-(2-hydroxyethyl) ammonium chloride (HEA16Cl) was prepared as previously described in the literature [34–36].

2.1.1. Supports

SBA-15 silica was synthesized according to the method reported by Zhao et al. [37]. In details, 4.0 g of P123 were dissolved at 40 °C in 140 mL of a HCl solution (1.7 mol L^{-1}). Then, 8.4 g of TEOS were added. The resulting gel was stirred at 40 °C for 24 h and hydrothermally treated in a fluorinated ethylene propylene (FEP) flask at 100 °C during 24 h. Finally, the solid was filtered, washed with water, dried at 80 °C overnight and calcined in air flow (flow = 30 mL min^{-1} , heating rate = $24 \text{ }^\circ\text{C h}^{-1}$) at 550 °C for 6 h.

Al-SBA-15, with a nominal Si/Al molar ratio of 10, was synthesized using the method described by Li et al. [38]. This material was prepared as follows: 4.0 g of P123 were dissolved in 150 mL of aqueous HCl (pH = 1.5) at 40 °C (solution A). Simultaneously, 6.4 mL of TMOS and 0.88 g of aluminium isopropoxide were added to 10 mL of aqueous HCl (pH = 1.5, solution B). Solution B was stirred at room temperature for 3 h and added dropwise to solution A. The resulting mixture was aged for 20 h at 40 °C and hydrothermally treated in a FEP flask at 100 °C for 24 h. The resulting solid was filtered, washed, dried and calcined at 550 °C for 5 h. The sodium form, Na-Al-SBA-15, was obtained by treating 1.0 g of calcined Al-SBA-15 solid by 100 mL of a 0.7 M NaCl solution at 80 °C for 48 h. Na-Al-SBA-15 solid was recovered by filtration, washed with distilled water and dried 24 h at 60 °C. The experimental Na/Al ratio was 0.5 [33].

The mesoporous carbon material, CMK-3, was prepared by using SBA-15 as template and sucrose as carbon source [39]. A solution, obtained by dissolving 1.25 g of sucrose and 0.14 g of 98 wt.% H_2SO_4 in 5.0 g of water, was contacted with 1.0 g of SBA-15. The resulting mixture was then treated at 100 °C for 6 h and at 160 °C for another 6 h. The recovered solid was impregnated again with a solution containing 0.8 g of sucrose, 0.09 g of 98 wt.% H_2SO_4 and 5.0 g of water, and was thermally treated as described above. Finally, the obtained composite material was pyrolyzed in nitrogen flow at 900 °C for 6 h (flow = 20 mL min^{-1} , heating rate = $300 \text{ }^\circ\text{C h}^{-1}$). CMK-3 was recovered by dissolving silica in 1 M aqueous/ethanol solution of NaOH (50 mL per 1.0 g of starting material). After 24 h, the solid was filtered, washed with absolute ethanol and dried at 80 °C during 12 h.

2.1.2. Rh(0) containing solids

The support (SBA-15, Na-Al-SBA-15 or CMK-3) (1.0 g) was dispersed in 25 mL of distilled water in the presence of HEA16Cl (0.063 g , $1.8 \cdot 10^{-4} \text{ mol}$) for 24 h. Then, rhodium(III) chloride hydrate (0.024 g) was contacted with the solid for 2 h. A pH adjustment to 9.5 (addition of a few drops of 30 wt.% aqueous NH_3) was necessary in the case of SBA-15 and CMK-3. Reduction occurred instantaneously after NaBH_4 (10 mg) introduction as shown by a colour change from yellow to black. After 2 h, the solid was filtered,

Table 1

Acronyms of the different Rh(0) based-solids.

Samples	Support	pH adjustment	HEA16Cl
Rh ⁰ -SBA-NH ₃	SBA-15	Yes	Yes
Rh ⁰ -SBA-NH ₃ (B)			No
Rh ⁰ -CMK-NH ₃	CMK-3	Yes	Yes
Rh ⁰ -CMK-NH ₃ (B)			No
Rh ⁰ -Na-AlSBA	Na-Al-SBA-15	No	Yes
Rh ⁰ -Na-AlSBA(B)			No

washed and dried at 60 °C for 24 h. Blank preparations were carried out on the three supports. The blank solids were synthesised using the procedure above but in the absence of HEA16Cl. Table 1 summarizes the acronyms of the different solids and gives some preparation details.

2.2. Materials characterization

The silicon, rhodium, carbon and nitrogen compositions of the various materials were determined by ICPAES in the CNRS analysis center at Vernaison (France). X-ray powder diffraction (XRD) data were recorded with a Bruker D8 Advance diffractometer using the Cu K α radiation in the 2θ range between 0.5° and 5°. N₂ adsorption-desorption isotherms were measured at liquid nitrogen temperature using a Micromeritics ASAP 2010 instrument. Before analysis, samples were degassed overnight at room temperature and 8 h at 200 °C. Specific surface areas were evaluated using the Brunauer-Emmett-Teller (BET) method in the P/P_0 range of 0.05–0.25. Pore sizes were determined using the Barrett-Joyner-Halenda (BJH) method applied to the desorption isotherms. Thermal analysis (TG-DSC) of Rh⁰-SBA-NH₃ was performed on a SDT 2960 system (TA Instruments, Inc.). Measurements were carried out in a constant (100 mL min^{-1}) N₂ flow with a heating rate of $10 \text{ }^\circ\text{C min}^{-1}$. Transmission electron microscopy (TEM) images were recorded with a JEOL TEM 100 CXII electron microscope operating at an acceleration voltage of 100 kV.

2.3. Catalysis test

Rh(0) containing solids were used as catalysts in the hydrogenation of styrene and diphenylmethane (99%, Aldrich). A weighted amount (50 mg) of the material was dispersed in hexane (10 mL) for 15 min prior to the introduction of the arene derivative (100 equiv. per eq metal). The tests were carried out at room temperature under 0.1 MPa H₂. Products were analysed with a Delsi Nermag gas chromatograph equipped with a Macherey-Nagel Optima[®]-5 capillary column and a FID detector. Quantifications were performed using n-decane as internal standard. Recycling test for Rh⁰-CMK-NH₃ (B) was performed after filtration and drying (60 °C) of the sample recovered from the first run. There was no activation step. Conditions for the second test were the same as those used for the fresh catalyst (see above).

3. Results and discussion

For all preparations, the nominal NaBH_4/Rh and HEA16Cl/Rh molar ratio used were rigorously the same as those of the optimized synthesis of 2–3 nm Rh(0) colloidal particles in aqueous solution [36] (i.e., 2.5 and 2, respectively). The theoretical value of rhodium loading onto the different supports was 1.0 wt.%. According to elemental analysis results reported in Table 2, Rh(III) uptake by the different supports is facilitated in the presence of the cationic stabilizing agent. Indeed, Rh loadings of samples prepared with HEA16Cl are between 1.5 and 3.5 times higher than those of the corresponding blank materials. Table 2 also indicates that the inser-

Table 2
Physicochemical properties of Rh⁰-containing samples.

Sample	Rh (wt.%)	N (wt.%)	S _{BET} (m ² g ⁻¹)	V _p (cm ³ g ⁻¹)	D _p (nm)
SBA-15	–	–	912	1.03	6.7
Rh ⁰ -SBA-NH ₃	0.55	0.2	495	0.99	7.6
Rh ⁰ -SBA-NH ₃ (B)	0.15	–	734	1.00	6.9
CMK-3	–	–	852	0.73	3.4
Rh ⁰ -CMK-NH ₃	0.96	0.2	653	0.57	3.3
Rh ⁰ -CMK-NH ₃ (B)	0.58	–	878	0.86	3.2
Na-Al-SBA-15	–	–	785	1.03	7.9
Rh ⁰ -Na-AlSBA	0.90	0.2	870	1.24	7.0
Rh ⁰ -Na-AlSBA(B)	0.40	–	795	0.99	8.2

tion of rhodium is more difficult on pure silica than on the other supports.

Differences in Rh loading, observed on blank samples (prepared in the absence of the stabilizing agent) may be understood by referring to a model based on electrostatic interactions between the negatively charged supports and Rh complexes in solution. Indeed, the pH of the solution was about 6 for Na-Al-SBA-15, 9 for SBA-15 and CMK-3 and reported isoelectric point values of pure silica, silica-alumina (5 wt.% Al₂O₃) and carbon are 2 [40], 2–5 [41] and 3–4 [42], respectively. In these conditions, it is conceivable that the cationic aqua (Na-Al-SBA-15) or ammine (SBA-15, CMK-3) rhodium complexes are adsorbed on the support through electrostatic interactions. Differences in rhodium uptake may be due to variations of the surface concentration of negative charges and thus of the nature of the support. In the specific case of Rh⁰-CMK-NH₃(B) sample, Rh content is in agreement with those of various activated carbons prepared by Daza et al. [43].

The systematic increase in Rh loading as the result of the addition of the cationic stabilizing agent may correspond to the formation of admicelles [44,45]. Hence quaternary ammonium groups of HEA16Cl molecules would potentially interact with negatively charged surfaces leading to adsorption and the formation of a bilayer through tail to tail interactions. Resulting admicelles would lead to Rh³⁺ uptake through NR₄⁺...Cl⁻...Rh³⁺ association [46]. Aqueous Rh(III) species would be adsorbed during the 2 h stirring period prior to the reduction step. Taking into account the fact that most of the polar heads of the surfactant are oriented to the solution, one admicelle could stabilize more Rh(III) species than one negative surface charge.

Thermogravimetric and elemental analyses of Rh⁰-Na-Al-SBA and Rh⁰-SBA-NH₃ samples are consistent with the presence of HEA16⁺ cations. Indeed, values of the molar C/N ratio in both solids are equal to 24. The slight difference between the theoretical and the experimental value could be due to some contamination by P123 (expected ratio of C/N is 20). Thermogravimetric studies of Rh⁰-Na-Al-SBA [33] and Rh⁰-SBA-NH₃ are also consistent with the presence of both molecules. Analysis of Rh⁰-SBA-NH₃ is similar to that of Rh⁰-Na-Al-SBA sample (Fig. 1).

The derivative of the thermogravimetric curve shows four peaks, at 65, 250, 350 and 540 °C, respectively. The first one corresponds to the desorption of physisorbed water. Others are associated to the decomposition of HEA16Cl and a residue of Pluronic P123 not eliminated by calcination at 550 °C [47,48]. In both cases, the overall percentage loss (physisorbed water not included) determined by TG analysis is about 8–9%. Elemental analysis would suggest the presence of 5 wt.% of HEA16Cl (based on nitrogen amount) and about 2% of Pluronic P123. Nitrogen loading of all Rh-based solids is 0.2 wt.% (0.14 mmol g⁻¹) whereas theoretical one is 0.24% (0.18 mmol g⁻¹). Actually, it can be concluded from elemental analysis of the different solids recovered after the reduction step, that c.a. 80% of the HEA16Cl contacted with the supports is adsorbed.

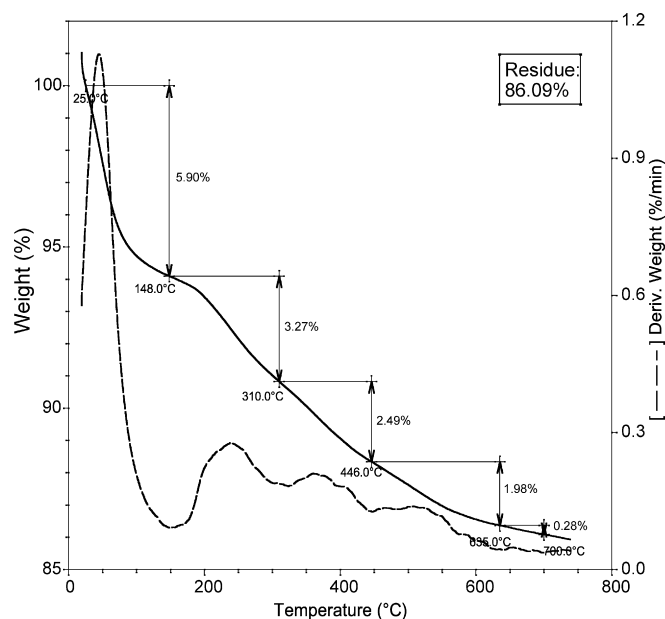


Fig. 1. Thermogravimetric analysis of Rh⁰-SBA-NH₃.

According to the above-mentioned data, all supports adsorbed approximately the same amount of HEA16Cl. However, rhodium uptake of pure silica support is inferior to those obtained with Na-Al-SBA-15 and CMK-3. So, it can be concluded that, even if HEA16Cl molecules play a determining role in the uptake of the rhodium species, the nature of the support is also very important. Such conclusion agrees with previous observations [33]. Indeed, we already showed that modification of Al-SBA-15 surface through H⁺/Na⁺ exchange induces an increase of the final Rh loading from 0.44 to 0.90 wt.%. Arrangement of the adsorbed surfactant molecules and, hence their ability to capture Rh(III) complexes, probably differ with the intrinsic nature of the support as well as with its textural properties.

3.1.1. Structural and textural characterizations of the materials

All samples are characterized by the three diffraction peaks ((100), (110) and (200)) attributed to a 2D-hexagonal structure and there was almost no change of the cell parameters upon Rh incorporation. The significant decrease of the intensities of the diffraction peaks observed in the particular case of Rh⁰-SBA-NH₃ and Rh⁰-SBA-NH₃(B) materials may be related to a partial dissolution of the silica support following the addition of ammonia (pH adjustment). Nitrogen adsorption-desorption isotherms of SBA-15 and Na-AlSBA-15-based materials (Fig. 2a and b) exhibit type IV isotherms with a H1 hysteresis loop characteristic of structured materials of the SBA-15 type.

Modification of the isotherms of the SBA-15-based solids upon rhodium incorporation (Fig. 2a) are related to a decrease of the specific surface area and an increase of the average pore diameter (Table 2) during the catalyst preparation. As proposed by Galarneau et al. [49], such modifications can be attributed to a partial solubilisation of the walls thus inducing the loss of the microporous component of the total surface area and an increase of the pore diameters. Textural properties of Rh⁰-Na-AlSBA and its corresponding blank material are not remarkably different from those of their parent, Na-AlSBA-15. A slight increase of specific surface area and pore volume was observed in the case of Rh⁰-Na-AlSBA. This sample is characterized by a deformation of its hysteresis loop in comparison with those of Na-Al-SBA-15 and Rh⁰-Na-AlSBA(B) (Fig. 2b).

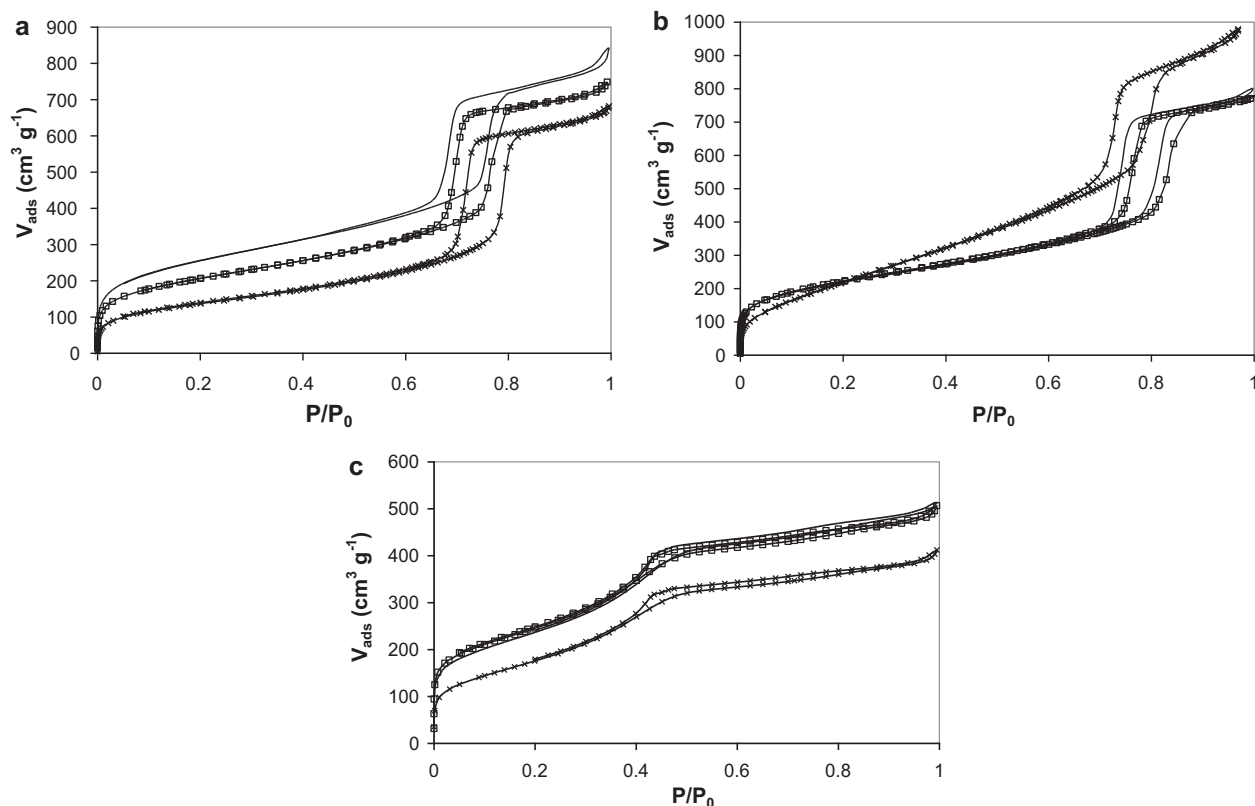


Fig. 2. N_2 adsorption-desorption isotherms of Rh(0) containing mesoporous materials and their supports at -196°C . (a) (–) SBA-15, (\square) Rh^0 -SBA- NH_3 (B) and (\times) Rh^0 -SBA- NH_3 (b) (–) Na-Al-SBA-15, (\square) Rh^0 -Na-AlSBA (B) and (\times) Rh^0 -Na-AlSBA. (c) (–) CMK-3, (\square) Rh^0 -CMK- NH_3 (B) and (\times) Rh^0 -CMK- NH_3 .

Isotherms of CMK-3 support and CMK-3-based samples (Fig. 2c) is of type IV with a H2 hysteresis loop characteristic of this type of mesoporous solids [39]. According to Fig. 2c and Table 2, CMK-3 and Rh^0 -CMK- NH_3 (B) samples have similar textural properties. However, Rh^0 -CMK- NH_3 , prepared with HEA16Cl, is characterized by lower surface area and pore volume. The important modification of the textural properties during the synthesis of Rh^0 -CMK- NH_3 cannot be explained only by the incorporation of the metallic nanoparticles. It could also be related to a filling up or a blocking of some pores by HEA16Cl molecules.

3.1.2. TEM study

Transmission electron microscopy analyses allowed to verify that pore channels of SBA-15 and CMK-3-based samples are still structured after NH_3 treatment. The absence of stabilizing agent molecules leads to a poor dispersion of Rh(0) in SBA-15 and Na-Al-SBA-15-based materials. As shown in Fig. 3b and d, significant amounts of Rh(0) nanoparticles are formed on the external surface of the SBA-15 and Al-SBA-15 solids. Rhodium is present as large particles (average

Table 3

Reactant distribution vs time in the catalytic hydrogenation of styrene with Rh(0) containing heterogeneous catalysts.

Samples	Rh (wt %)	3 h		6 h			
		Styrene conv. (%) [T.O.N.] ^a	Sel. (%)		Styrene conv. (%) [T.O.N.]	Sel. (%)	
			EB	EC		EB	EC
Rh^0 -Na-AlSBA	0.90	100[400]	0	100	100[400]	0	100
Rh^0 -Na-AlSBA (B)	0.40	100[256]	48	52	100[400]	0	100
Rh^0 -SBA- NH_3	0.55	100[202]	66	34	100[400]	0	100
Rh^0 -SBA- NH_3 (B)	0.15	100[229]	57	43	100[400]	0	100
Rh^0 -CMK- NH_3	0.96	100[229]	57	43	100[355]	15	85
Rh^0 -CMK- NH_3 (B)	0.58	100[310]	30	70	100[400]	0	100
Rh^0 -CMK- NH_3 (B) ^b	n.d.	100[277]	41	59	100[394]	2	98
Rh^0/SiO_2 ^c	1	99[174]	75	25	99[243]	51.5	48.5
Rh^0/C ^c	1	97[118]	93	7	99[144]	85	15
Commercial Rh^0/C ^d	5	0[0]	–	–	98[146]	84	16

Conditions. Catalyst (50 mg), hexane (10 mL), $T = 25^\circ\text{C}$, $P(\text{H}_2) = 0.1 \text{ MPa}$, substrate/Rh = 100.

^a T.O.N. expressed as number of mol of H_2 consumed per number of mol of Rh.

^b Recycled catalyst.

^c Samples synthesized by incipient wetness impregnation of SiO_2 (Aerosil 200) or activated carbon (Bioinvest) by aqueous RhCl_3 followed by a reduction step treatment under H_2 at 220°C .

^d Supplied by Aldrich.

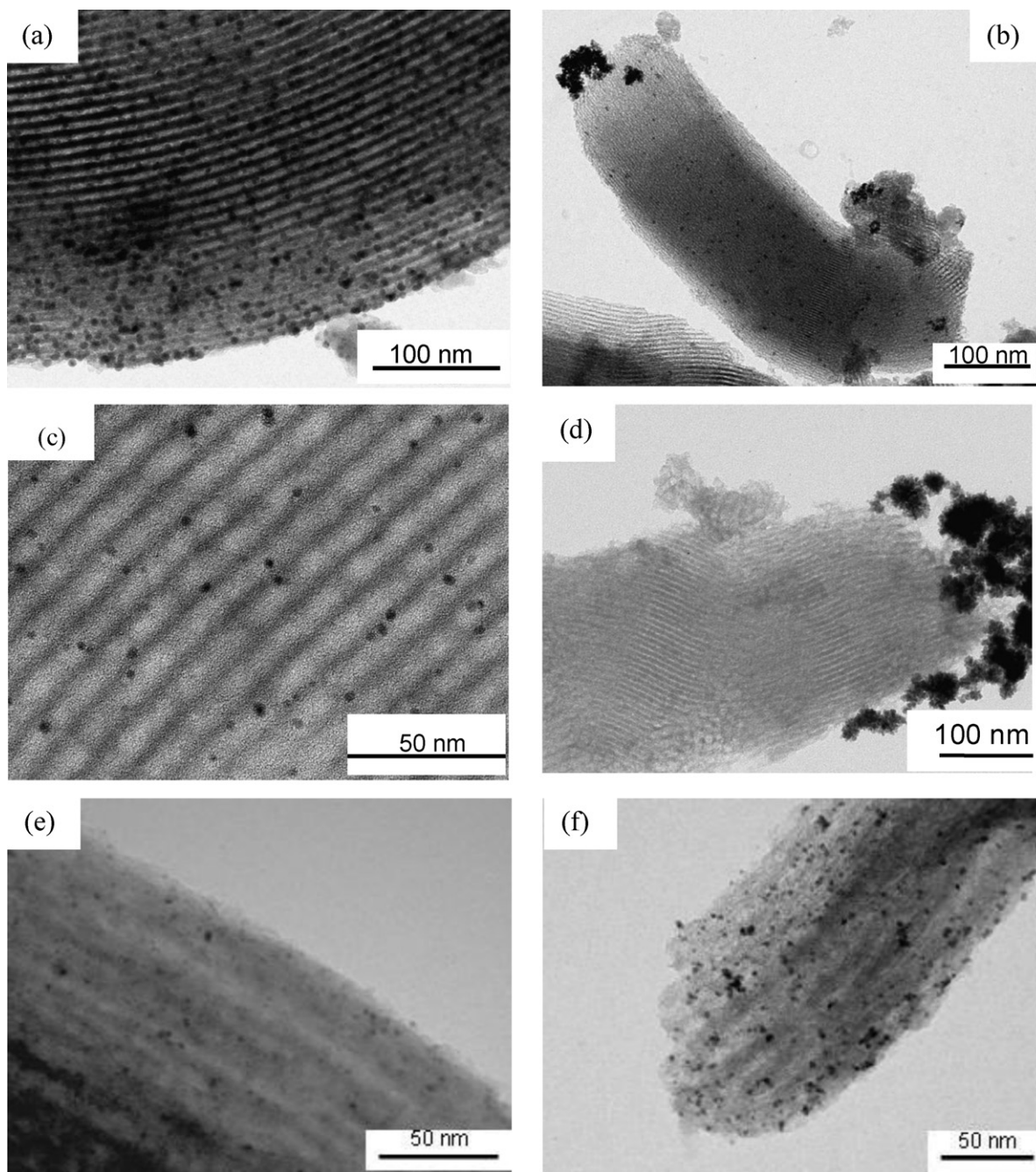


Fig. 3. TEM images of (a) $\text{Rh}^0\text{-SBA-NH}_3$, (b) $\text{Rh}^0\text{-SBA-NH}_3$ (B), (c) $\text{Rh}^0\text{-Na-AISBA}$, (d) $\text{Rh}^0\text{-Na-AISBA}$ (B), (e) $\text{Rh}^0\text{-CMK-NH}_3$ and (f) $\text{Rh}^0\text{-CMK-NH}_3$ (B) samples.

diameter = 7 nm for $\text{Rh}^0\text{-SBA-NH}_3$ (B), Fig. 3b) or aggregates (Fig. 3b and d).

The use of HEA16Cl induces the presence of larger amounts of small nanoparticles located inside the mesopore channels (average diameter = 5 and 3 nm for $\text{Rh}^0\text{-SBA-NH}_3$ and $\text{Rh}^0\text{-Na-AI-SBA}$, respectively, Fig. 3a and c). Small aggregates on the external surface (not shown) are still observed but to a lesser extent than in the absence of HEA16Cl. In general, Rh(0) particles formed on CMK-3 solids (Fig. 3e and f) are smaller than those observed on the two other supports (Fig. 3a–d). Size distribution histograms of the particles in samples prepared with HEA16Cl are presented in Fig. 4. Clearly, the best metal dispersion is

obtained on CMK-3. Histograms of the silica-based materials show a narrow size distribution centred at 3–4 nm for $\text{Rh}^0\text{-Na-AISBA}$ and a broader one centred at 6–7 nm for $\text{Rh}^0\text{-SBA-NH}_3$. In the case of $\text{Rh}^0\text{-CMK-NH}_3$ and $\text{Rh}^0\text{-SBA-NH}_3$, the mean diameters of the particles are very close to the pore aperture of the support, i.e., 3 and 6 nm, respectively.

In conclusion, TEM studies have shown that the use of HEA16Cl facilitates the preparation of well-dispersed Rh(0) nanoparticles. Indeniably, the size of the nanoparticles prepared with similar NaBH_4/Rh ratio is influenced by the pore aperture of the mesoporous supports (6.7, 3.4 and 7.9 nm for SBA-15, CMK-3 and Na-AI-SBA-15, respectively). However, the average size of the

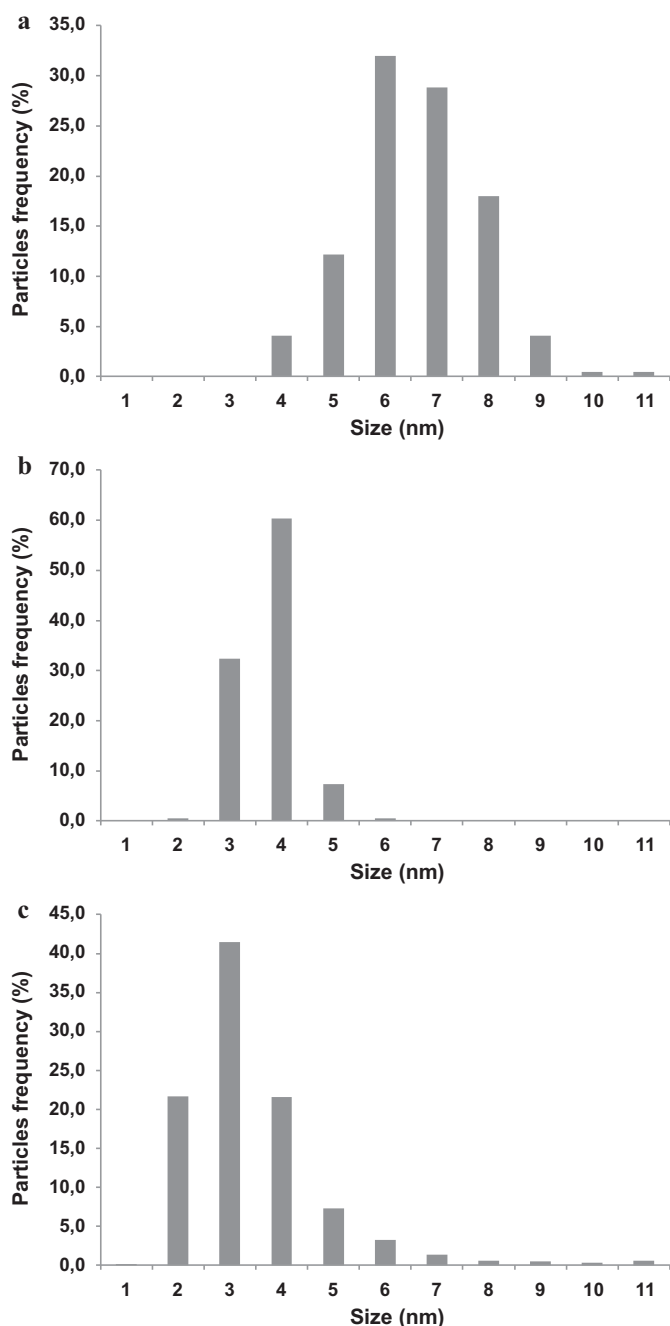
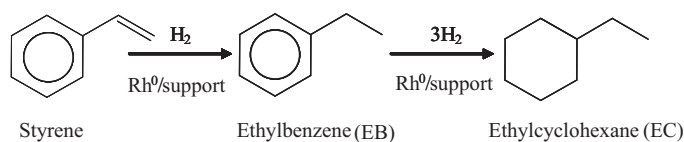


Fig. 4. Nanoparticles size distribution histograms in (a) Rh⁰-SBA-NH₃, (b) Rh⁰-Na-AISBA and (c) Rh⁰-CMK-NH₃ samples.

colloids formed in Na-Al-SBA-15 is smaller than the average mesopore diameter which implies that a greater control is exercised by HEA16Cl on this support.

3.1.3. Catalytic performance of the materials

The conversion of aromatic cycles into cyclohexyl groups is a goal of important interest both at the industrial or laboratory scale [50–52]. Formation of cyclohexane from benzene for adipic acid synthesis or removal of aromatic derivatives from fuels are mainly performed in the presence of Ni and Pt-based catalysts under harsh conditions [53]. Ru or Rh based materials represent convenient alternatives [52,54–58]. They can work under milder conditions and are particularly adapted to the synthesis of fine



Scheme 1.

chemicals. We previously showed that Rh⁰-Na-AISBA efficiently catalyze the hydrogenation of various aromatic substrates (styrene, anisole, toluene, m-xylene and tetralin) at room temperature at atmospheric pressure of dihydrogen [33]. The aim of the present study is to look at the influence of the support (Na-Al-SBA-15, SBA-15 and CMK-3) as well as of the use of HEA16Cl. Comparative tests were performed with styrene (Table 3) and diphenylmethane (Table 4).

The reaction was carried out with similar substrate/Rh molar ratio (1/00) in hexane. Such conditions correspond to those used in the case of non supported Rh(0) colloids stabilized by HEA16Cl [36]. Whatever the catalyst considered, the external double bond of styrene was more easily reduced than the aromatic ring of the molecules (Scheme 1). Ethylcyclohexane (EC) and the intermediate, ethylbenzene (EB), are the only products obtained.

All the Rh(0) containing mesoporous materials turned out to be much more active than either commercial Rh⁰/C or conventionally synthesized reference catalysts (Rh⁰/SiO₂, Rh⁰/C). Excepted for Rh⁰-CMK-NH₃ sample, complete conversion of styrene into ethylcyclohexane was reached in less than 6 h. Most active catalysts are Rh⁰-Na-AISBA and Rh⁰-CMK-NH₃(B). The efficiency of SBA-15-based solids does not depend on the presence or absence of HEA16Cl. The quite low activity of Rh⁰-SBA-NH₃ and Rh⁰-SBA-NH₃(B) can be understood as the result of the presence of a lot of aggregates on the external surface as well as particles with larger average sizes in these samples.

Differences between HEA16Cl-containing samples and blank ones are more significant but contradictory in the cases of Na-Al-SBA-15 and CMK-3 supports. With Rh⁰-CMK-NH₃, ethylcyclohexane yield was 85% after 6 h. The lower activity of Rh⁰-CMK-NH₃ compared to that of Rh⁰-CMK-NH₃(B) can be interpreted by the steric hindrance induced by HEA16Cl molecules surrounding Rh(0) nanoparticles in a limited volume space (D_p of CMK-3 is 3.4 nm). Indeed, it has to be noted that the total pore volume of CMK-3 has been strongly decreased (by ≈20%) when HEA16Cl was used. Variations were weaker for Na-Al-SBA-15 supports. As the result, lower performance of Rh⁰-CMK-NH₃ compared to Rh⁰-Na-AISBA could be explained by the low diffusion rate of styrene molecules to the surface of Rh(0) nanoparticles.

Previously, it was shown that the activity of Rh⁰-Na-AISBA is not affected significantly over three successive tests [33]. In the present study, despite a little bit slower reaction kinetic, Rh⁰-CMK-NH₃(B) recovered from the first test was shown to be still efficient in a second run (Table 3) carried out under similar conditions (ethylcyclohexane yield = 98% instead of 100% after 6 h). The rate decrease observed is probably due to partial leaching of rhodium.

Given that Rh⁰-Na-AISBA and Rh⁰-CMK-NH₃ samples are characterized by similar dispersions and particles sizes, it can be concluded that differences in the catalytic activity observed are related to the average pore diameters of the supports. Changes in the nature of the interaction of HEA16Cl with the surfaces of the support and of the metal particles could also be mentioned.

Catalytic performances of Rh⁰-Na-AISBA and Rh⁰-CMK-NH₃(B) samples are a little bit lower than those of the Rh(0) colloids stabilized by HEA16Cl [33,36]. Comparisons with other heterogeneous catalytic systems based either on Rh(0) nanoparticles or Rh complexes are not easy. Reported

Table 4
Reactant distribution vs time in the catalytic hydrogenation of diphenylmethane with Rh(0) containing heterogeneous catalysts.

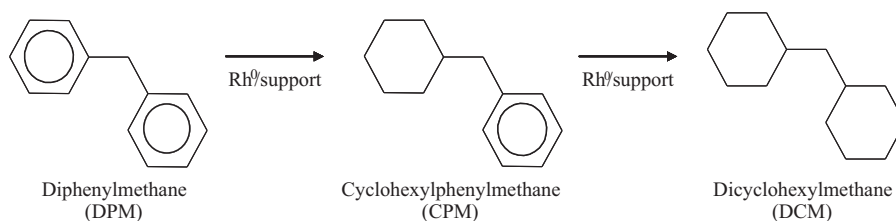
Samples	Rh (wt.%)	6 h			24 h		
		DPM conv. (%) [T.O.N.] ^a	Sel. (%)		DPM conv. (%) [T.O.N.]	Sél. (%)	
			CPM	DCM		CPM	DCM
Rh ⁰ -Na-AlSBA	0.90	51[195]	72.5	27.5	99[588]	2	98
Rh ⁰ -Na-AlSBA (B)	0.40	13[39]	100	0	46[180]	69.5	30.5
Rh ⁰ -CMK-NH ₃	0.96	48[162]	87.5	12.5	93[351]	74	26
Rh ⁰ -CMK-NH ₃ (B)	0.58	67[237]	82	18	100[600]	0	100
Rh ⁰ /SiO ₂ ^b	1	27[90]	89	1	86[324]	74	26
Rh ⁰ /C ^c	1	2[6]	100	0	15[51]	87	13
Commercial Rh ⁰ /C ^c	5	0[0]	0	0	5[18]	80	20

Conditions. Catalyst (50 mg), hexane (10 mL), $T = 25^\circ\text{C}$, $P(\text{H}_2) = 0.1\text{ MPa}$, substrate/Rh = 100.

^a T.O.N. expressed as number of mol of H₂ consumed per number of mol of Rh.

^b Samples synthesized by incipient wetness impregnation of SiO₂ (aerosil 200) or activated carbon (Bioinvest) by RhCl₃·xH₂O followed by reduction under H₂ at 220 °C.

^c Aldrich.



Scheme 2.

experiments are often performed at higher H₂ pressure (0.5 MPa) or at higher temperature (60 °C). Solvents are not always the same. Buil et al. [54] recently described the preparation of 2 wt.% Rh(0)/Al₂O₃ from the reduction of a Rh(I) complex in the presence of Al₂O₃. Hydrogenation of the exocyclic double bond was very efficient but, despite less difficult catalysis test conditions (Substrate/Rh = 50, $T = 60^\circ\text{C}$), such material was not able to allow the complete hydrogenation of styrene into ethylcyclohexane within 4 h (T.O.N. = 70).

Hydrogenation of diphenylmethane (DPM), into dicyclohexylmethane (DCM) (Scheme 2) was also investigated under similar conditions. Na-Al-SBA-15 and CMK-3-based solids were tested in comparison with Rh⁰/SiO₂, Rh⁰/C and commercial Rh⁰/C. Whatever the test considered, cyclohexylphenylmethane (CPM) was observed as a reaction intermediate.

Diphenylmethane is a more demanding substrate as corroborated by the low conversion of DPM after 24 h in the presence of the reference materials and Rh⁰-Na-AlSBA(B) (Table 4).

Total or quasi-total conversion of DPM into DCM was observed with the best catalysts for styrene hydrogenation. Actually, performances of Rh⁰-Na-AlSBA and Rh⁰-CMK-NH₃(B) samples compare well with those of other reported catalytic materials. For example, Maegawa et al. [52] recently described the use of Rh(0)/C as a catalyst to get DCM from DPM. It has to be noted that best conditions (isopropanol as the solvent, $T = 60^\circ\text{C}$, $P = 0.5\text{ MPa}$ and a substrate/Rh = 10) are more drastic than ours. In our case, influences of the particles size and of the properties of the support on the catalytic activity are shown again. Moreover, larger differences between the activities of Rh⁰-CMK-NH₃ and Rh⁰-CMK-NH₃(B) for CPM hydrogenation compared to styrene emphasize the importance of the steric hindrance induced by HEA16Cl around Rh(0) nanoparticles in CMK-3.

4. Conclusions

Heterogeneously nucleated rhodium (0) colloids were prepared on various mesoporous materials by reproducing the previously

described protocol involving Na-Al-SBA-15 and HEA16Cl as a stabilizing agent [33]. In this study, it is clear that, whatever the support (silica, aluminosilica or carbon), prior adsorption of the quaternary ammonium salt then facilitates that of rhodium (III). According to elemental and thermogravimetric analyses, nearly 80% of the initial amount of the stabilizing agent is retained by the solids. The increase in adsorption capacity of the resulting materials is a priori related to admicellisation phenomena. These however seem to vary from one sample to another. In all cases, the nature of the support is the determining factor. Indeed, adsorption capacities with and without HEA16Cl are classified in the same order.

Generally, metal nanoparticles prepared in the presence of HEA16Cl are smaller and more dispersed at least on the silicic and aluminosilic materials of the SBA-15 type. In the case of CMK-3, particle size is controlled by the average pore diameter and HEA16Cl present on the solid reduces the catalytic activity. Nevertheless, all Rh(0)-based materials prepared in this study are much better catalysts in the hydrogenation of aromatic rings than commercial analogues tested under the same conditions ($P_{\text{H}_2} = 0.1\text{ MPa}$ and ambient temperature). Further studies of the Na-Al-SBA-15/HEA16Cl system are in progress in order to better understand interactions of HEA16Cl with Na-Al-SBA-15 as well as to take advantage of the latter to develop new selectivities.

References

- [1] G. Schmid, L. Chi, *Adv. Mater.* 10 (1998) 515–526.
- [2] G. Schmid, M. Baumle, M. Geerkens, I. Heim, C. Osemann, T. Sawitowski, *Chem. Soc. Rev.* 28 (1999) 179–185.
- [3] J.D. Aiken III, R.G. Finke, *J. Mol. Catal. A: Chem.* 145 (1999) 1–44.
- [4] A. Roucoux, J. Schulz, H. Patin, *Chem. Rev.* 102 (2002) 3757–3778.
- [5] B.L. Cushing, C.J. Kolesnichenko, C.J. O'Connor, *Chem. Rev.* 104 (2004) 3893–3946.
- [6] F. Kleitz, in: G. Ertl, H. Knözinger, F. Schüth, J. Weitkamp (Eds.), *Handbook of Heterogeneous Catalysis*, vol. 1, 2nd ed., Wiley-VCH, Weinheim, 2008, pp. 168–219.
- [7] W.J. Roth, J.C. Vartuli, *Stud. Surf. Sci. Catal.* 157 (2005) 91–110.
- [8] C. Li, H. Zhang, D. Jiang, Q. Yang, *Chem. Commun.* (2007) 547–558.
- [9] F. Goettmann, C. Sanchez, *J. Mater. Chem.* 17 (2007) 24–30.
- [10] J.H. Clark, D.J. MacQuarrie, S.J. Tavener, *Dalton Trans.* 35 (2006) 4297–4309.

- [11] A. Corma, H. Garcia, *Adv. Synth. Catal.* 348 (2006) 1391–1412.
- [12] F.-S. Xiao, *Top. Catal.* 35 (2005) 9–24.
- [13] A. Vinu, K.Z. Hossain, K. Ariga, *J. Nanosci. Nanotechnol.* 5 (2005) 347–371.
- [14] J.M. Thomas, R. Raja, *J. Organomet. Chem.* 689 (2004) 4110–4124.
- [15] A. Taguchi, F. Schueth, *Micropor. Mesopor. Mater.* 77 (2004) 1–45.
- [16] A. Beck, A. Horváth, Gy. Stefler, R. Katona, O. Gesztö, Gy. Tolnai, L.F. Liotta, L. Guzzi, *Catal. Today* 139 (2008) 180–187.
- [17] É. Molnár, G. Tasi, Z. Kónya, I. Kiricsi, *Catal. Lett.* 101 (2005) 159–167.
- [18] É. Molnár, Z. Kónya, G. Tasi, I. Kiricsi, *Stud. Surf. Sci. Catal.* 158 (2005) 1351–1358.
- [19] R.M. Rioux, H. Song, J.D. Hoefelmeyer, P. Yang, G.A. Somorjai, *J. Phys. Chem. B* 109 (2005) 2192–2202.
- [20] G.A. Somorjai, J.Y. Park, *Top. Catal.* 49 (2008) 126–135.
- [21] J.N. Kuhn, W.Y. Huang, C.K. Tsung, Y.W. Zhang, G.A. Somorjai, *J. Am. Chem. Soc.* 130 (2008) 14026–14027.
- [22] A. Quintanilla, V.C.L. Butselaar-Orthlieb, C. Kwakernaak, W.G. Sloof, M.T. Kreutzer, F. Kapteijn, *J. Catal.* 271 (2010) 104–114.
- [23] J.N. Kuhn, C.-K. Tsung, W. Huang, G.A. Somorjai, *J. Catal.* 265 (2009) 209–215.
- [24] J. Zhu, Z. Kónya, V.F. Puentes, I. Kiricsi, C.X. Miao, J.W. Ager, A.P. Alivisatos, G.A. Somorjai, *Langmuir* 19 (2003) 4396–4401.
- [25] J.P.M. Niederer, A.B.J. Arnold, W.F. Hölderich, B. Spliethof, B. Tesche, M. Reetz, H. Bönemann, *Top. Catal.* 18 (2002) 265–269.
- [26] H. Song, R.M. Rioux, J.D. Hoefelmeyer, R. Komor, K. Niesz, M. Grass, P. Yang, G.A. Somorjai, *J. Am. Chem. Soc.* 128 (2006) 3027–3037.
- [27] Z. Kónya, V.F. Puentes, I. Kiricsi, J. Zhu, J.W. Ager, M.K. Ko, H. Frei, A.P. Alivisatos, G.A. Somorjai, *Chem. Mater.* 15 (2003) 1242–1248.
- [28] S. Chytil, W.R. Glomn, E. Vollebakk, H. Bergem, J. Walmesly, J. Sjöblom, E.A. Blekkan, *Micropor. Mesopor. Mater.* 86 (2005) 198–206.
- [29] M.E. Grass, S.H. Joo, Y.W. Zhang, G.A. Somorjai, *J. Phys. Chem. C* 113 (2009) 8616–8623.
- [30] C. Aprile, A. Abad, H. Garcia, A. Corma, *J. Mater. Chem.* 15 (2005) 4408–4413.
- [31] R. Mouawia, M. Boutros, F. Launay, V. Semmer-Herledan, A. Gedeon, V. Mevellec, A. Roucoux, *Stud. Surf. Sci. Catal.* 158 (2005) 1573–1580.
- [32] J. Ding, K.-Y. Chan, J. Ren, F.-S. Xiao, *Electrochim. Acta* 50 (2005) 3131–3141.
- [33] M. Boutros, A. Denicourt-Nowicki, A. Roucoux, L. Gengembre, P. Beaunier, A. Gedeon, F. Launay, *Chem. Commun.* (2008) 2920–2922.
- [34] J. Schulz, A. Roucoux, H. Patin, *Chem. Eur. J.* 6 (2000) 618–624.
- [35] J. Schulz, S. Levigne, A. Roucoux, H. Patin, *Adv. Synth. Catal.* 344 (2002) 266–269.
- [36] J. Schulz, A. Roucoux, H. Patin, *Adv. Synth. Catal.* 345 (2003) 222–229.
- [37] D. Zhao, J. Feng, Q. Huo, N. Melosh, G.H. Frederickson, B.F. Chmelka, *Science* 279 (1998) 548–552.
- [38] Y. Li, W. Zhang, L. Zhang, Q. Yang, Z. Wei, Z. Feng, C. Li, *J. Phys. Chem. B* 108 (2004) 9739–9744.
- [39] S. Jun, S.H. Joo, R. Ryoo, M. Kruk, M. Jaroniec, Z. Liu, T. Ohsuna, O. Terasaki, *J. Am. Chem. Soc.* 122 (2000) 10712–10713.
- [40] G.A. Parks, *Chem. Rev.* 65 (1965) 177–198.
- [41] X. Liu, Y. Hu, Z. Xu, *J. Colloid Interface Sci.* 267 (2003) 211–216.
- [42] S. Rondon, W.R. Wilkinson, A. Proctor, M. Houalla, D.M. Hercules, *J. Phys. Chem.* 99 (1995) 16709–16713.
- [43] L. Daza, T. Gonzalez Ayuso, S. Menidioroz, J.A. Pajares, *Appl. Catal.* 13 (1985) 295–304.
- [44] Z. Li, L. Gallus, *Colloid. Surf. A* 264 (2005) 61–67.
- [45] M.J. Meziani, J. Zajac, S. Partyka, *Langmuir* 16 (2000) 8410–8418.
- [46] B. Veisz, Z. Király, *Langmuir* 19 (2003) 4817–4824.
- [47] A.C.S.L.S. Coutinho, A.S. Quintella, A.S. Araujo, J.M.F. Barros, A.M.G. Pedrosa, V.J. Fernandes Jr., M.J.B. Souza, *J. Therm. Anal. Calorim.* 87 (2007) 457–461.
- [48] L. Xiao, J. Li, H. Jin, R. Xu, *Micropor. Mesopor. Mater.* 96 (2006) 413–418.
- [49] A. Galarneau, M. Nader, F. Guenneau, F. Di Renzo, A. Gedeon, *J. Phys. Chem. C* 111 (2007) 8268–8277.
- [50] B.R. James, Y. Wang, T.Q. Hu, *Chem. Ind.* 68 (1996) 423–428.
- [51] F. Glorius, *Org. Biomol. Chem.* 3 (2005) 4171–4175.
- [52] T. Maegawa, A. Akashi, K. Yaguchi, Y. Iwasaki, M. Shigetura, Y. Monguchi, H. Sajiki, *Chem. Eur. J.* 15 (2009) 6953–6963.
- [53] J. Cosyns, G. Martino, *Techniques de l'ingénieur*, J5500 1–18.
- [54] M.L. Buil, M.A. Esteruelas, S. Niembro, M. Oliván, L. Orzechowski, C. Pelayo, A. Vallribera, *Organometallics* 29 (2010) 4375–4383.
- [55] G.S. Fonseca, A.P. Umpierre, P.F.P. Fichtner, S.R. Teixeira, J. Dupont, *Chem. Eur. J.* 9 (2003) 3263–3269.
- [56] I.S. Park, M.S. Kwon, N. Kim, J.S. Lee, K.Y. Kang, J. Park, *Chem. Commun.* (2005) 5667–5669.
- [57] H. Yang, H. Gao, R.J. Angelici, *Organometallics* 19 (2000) 622–629.
- [58] H. Gao, R.J. Angelici, *New J. Chem.* 23 (1999) 633–640.